October 22, 1992

REACTOR PHYSICS TESTS OF TRIGA MARK-II REACTOR IN LJUBLJANA

M.Ravnik, I.Mele, A.Trkov, J.Rant, B.Glumac and V.Dimic

J.Stefan Institute, Jamova 39, Ljubljana, Slovenia
Tel.: 61 371-321
Fax: 61 374-919
Tlx: 31-296 yu jostin

University of Ljubljana
Institute "Jožef Stefan", Slovenia
Reactor Physics Division

1 INTRODUCTION

TRIGA Mark-II Reactor in Ljubljana was recently reconstructed. The reconstruction consisted mainly of replacing the grid plates, the control rod mechanisms and the control unit. The standard type control rods were replaced by the fuelled follower type, the central grid location (A ring) was adapted for fuel element insertion, the triangular cutouts were introduced in the upper plate design. However, the main novelty in reactor physics and operational features of the reactor was the instalation of a pulse rod. Having no previous operational experience in pulsing, a detailed and systematic sequence of tests was defined in order to check the predicted design parameters of the reactor with measurements. The following experiments are treated in this paper: initial criticality, excess reactivity measurements, control rod worth measurement, fuel temperature distribution, fuel temperature reactivity coefficient, pulse parameters measurement (peak power, prompt energy, peak temperature). Flux distributions in steady state and pulse mode were measured as well, however, they are treated only briefly due to the volume of the results. The experiments were performed with completely fresh fuel of 12 w% enriched Standard Stainless Steel type. The core configuration was uniform (one fuel element type, including fuelled followers) and compact (no irradiation channels or gaps), as such being particularly convenient for testing the computer codes for TRIGA reactor calculations. Comparison of analytical predictions, obtained with WIMS, SIXTUS, TRIGAP and PULSTRI codes to measured values showed agreement within the error of the measurement and calculation.

2 STEADY STATE EXPERIMENTS

2.1 Core loading and critical experiment

The nuclear instrumentation was tested before the experiment. Two additional BF_3 detectors were installed so that three independent source range neutron signals were available for $1/M$ measurements. Reactivity computer was connected to the linear channel. Critical experiment was started with completely empty core except for neutron source in F-12 and control rods (fuelled followers). Fuel was loaded from the centre (A ring) to the periphery, filling all positions in a ring before proceeding to the next. According to our calculations /1/ criticality was expected at approximately 40 fuel elements (including 3 fuelled followers). It was planned to insert fuel elements in E-ring into the locations near the transient rod. Criticality was closely approached (- 125 pcm) with 7 fuel elements in E-ring from E-4 to E-10 (total 43 fuel elements including fuelled followers, equivalent to 2355 g U-235). However, adding one more element would increase reactivity by more than 500 pcm and core excess reactivity would be too high to be measured directly from the period with all control rods withdrawn. In order to increase reactivity it was decided to replace fuel elements which contain less U-235 by those that contain more uranium (variations between elements are approx. 1 g U-235 according to fabrication specifications by General Atomics). Total weight of U-235 in the reactor was increased by $\approx$ 10 g, at least according to the documentation from where the data were taken. However, an increase in reactivity was not observed, ρ = - 135 pcm was measured.

Another effect was sought to increase reactivity to criticality without adding more fuel elements. It was decided to reshuffle all 7 fuel elements in E-ring from locations near transient rod to the opposite side (core no. 133, Fig. 1). It was expected that the flux distribution would be shifted and the importance of transient rod air follower would become smaller resulting in an increase of reactivity. Excess reactivity of $\approx$ 200 pcm was measured after reshuffling, confirming our assumptions and meeting acceptance criteria (compact core, less than 3 $ excess reactivity) as well as review criteria (excess reactivity between 10 - 200 pcm) for the test.

2.2 Flux range determination for tests at zero power

The purpose of this test was to determine flux level on log and linear channel above which temperature feedback effects would be observed. Linear channel reading was taken from the amplifier which is part of the reactivity computer system. Flux was allowed to increase with a constant period of about 100 s from approx. 6 pA (subcritical) to approx. 0.4 μA where nuclear heating was observed from drop in reactivity and from the shape of the trace of the log channel signal. 1-20 nA range

was selected for zero power tests. Later results of thermal calibration experiment showed that 0.4 μA corresponded to approx. 0.36 kW thermal power.

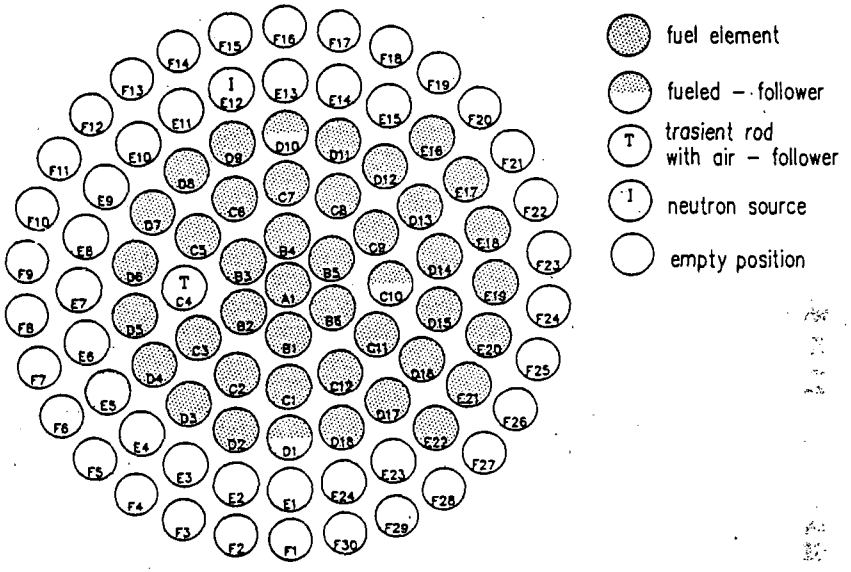

Fig. 1: Core no.133 (266 pcm excess reactivity, $T_W = T_F = 22.5°C$)

2.3 Digital reactivity meter checkout

The purpose of this test was to check proper functioning of the digital reactivity meter (DRM) by comparing reactivity, measured by DRM, to reactivity measured by the doubling-time method. Three different step reactivity changes were measured ($\approx$ 30, 70 and 80 pcm), maximal relative difference between DRM and doubling-time result was 2.6 % (or .8 pcm absolute). No overshoots, undershoots or drifts in DRM reactivity signal were observed, indicating perfect functioning of DRM as well as extremely good experimental conditions (stable temperature, no xenon, small gamma background). Acceptance criteria (15 % maximal and 10 % average error) were easily met.

2.4 Control rod worth measurements

Control rod worths were measured for all rods: regulating (R), compensating (C), transient (T) and safety (S). Rod insertion method was applied. Each rod was measured in the following way:

- Reactor was made approximately critical, all rods were withdrawn except one, compensating the excess reactivity. Safety rod was used to compensate excess reactivity (at ≈ 300 steps), except when its own worth was measured. In this case the excess reactivity was compensated simultaneously by regulating and compensating rod, both at 330 steps. Both rods were used to preserve flux symmetry as it was evident already from critical experiment that fuel element and control rod worths depend significantly on radial flux perturbations.

- Neutron flux signal storage was initiated on a disc file of the DRM system. Measured rod was moved from its completely withdrawn to completely inserted position with normal speed (≈ 4 min regulating and ≈ 1 min. any other rod). Start and end of travel were labelled on the disc file.

- After approx. 30 sec. with reactor deeply subcritical, the control rod was withdrawn with normal speed. Criticality was restored and data storage terminated.

- Differential and integral rod worth was calculated off-line from the flux signal using inverse point kinetics equation with source term (for detailed description of the method see ref. /2/).
  Results of the measurement are presented in Table I.

Table I: Control rod worths measured by rod insertion method, core 133

Rod	Worth [$\%\Delta\rho$]
regulating	1.9
compensating	1.5
safety	5.4
transient	1.9
Total:	10.7

The sum of regulating, compensating and safety rod is 8.8 $\%\Delta\rho$ or 12.6 \$. This value significantly exceeds acceptance criterion (4 \$) which is set with respect to alowed excess reactivity and required shutdown margin. It may be noted that the requirement is met even taking into account safety rod only. However, considering the results from reactor physics aspect, the following conclusions must be respected:

- Due to the symmetry of the core (See Fig. 1) and the same physical design of regulating and compensating rod their values should be very similar. Difference of .4 $\%\Delta\rho$ is observed.

  It may be attributed to the experimental error, unexpected asymmetry in the flux distribution in the core, or the inherent inaccuracy of the rod insertion method, as applied in this particular case. The first possibility was eliminated by repeating the measurement several times. Any strong asymmetry in the flux distribution could also be ruled out in view of the flux map results. The effect of the neutron source has also been considered by repeating the measurement with the source moved to the symmetric location E-7. Furthermore, the subsequent rod worth measurements by the rod-swap method give similar values for the *regulating and the compensating rod. The reason for the discrepancy must* therefore be sought in the rod insertion method itself.

  The rod insertion method is based on the point kinetics equations. It requires that the measured neutron signal is representative of the integral of the neutron flux. Since the flux signal is measured by an ionization chambers outside reactor core, this may not be a good assumption, particularly when the neutron flux distribution is significantly distorted. This effect is very strong in the case of the regulating rod which enters the core relatively closely the neutron detector connected to DRM, and less for the other rods. The flux redistribution effect is well known from the measurements at the Krško NPP. There the problem has been avoided by correcting the measured flux for the redistribution effect. The flux correction parameters require 2D adjoint transport calculation results which were not available for the TRIGA core. Therefore the control rod worth measurements presented do not include any corrections due to flux redistribution effects, what is reflected quite strongly in the large difference between the measured regulating and compensating rod worth by the rod insertion method.

- Physical design of all three control rods is the same. However, safety rod worth is ≈ 3 times greater than, e.g., compensating rod worth. Reason for such difference is the small importance of regulating and compensating rod positions at the periphery of the core, which itself is also very small. The results per se are not very surprising but indicate, that the rod worth may change also by a factor of two in other core configurations and that control rod worth measurements must be performed after every change in core configuration.

- Transient rod worth is relatively small (1.9 % or 2.7 \$) because the flux distribution is shifted towards fuel elements in the E ring.

Summarizing the last two conclusions it was decided to add new fuel elements for increasing excess reactivity to 3 \$ in E ring symmetrically near regulating and compensating rod and to reshuffle the rest of fuel elements in E ring (see core 134).

2.5 Excess reactivity measurement

Excess reactivity was measured directly from reactor period at all control rods withdrawn. Excess reactivity $\rho = 266$ pcm was measured for core no. 133. The influence of the source on reactivity was investigated. Removing of the source from E-12 increased excess reactivity of the core no. 133 by 44 pcm. This was measured by withdrawing the source from approx. critical reactor (excess reactivity was compensated by safety rod) using reactivity computer. The effect of the source on reactivity was expected since it had also been observed in the previous cores (before reconstruction). Negative effect of the source on reactivity is a result of reduced moderation as it displaces water. To investigate the symmetry of the core we inserted the source also in E-2, which is the "mirror" location of E-12 in the core 133. Excess reactivity was not changed. To achieve complete symmetry of the core, the source was finaly inserted into E-7. Excess reactivity of such configuration (133 A) was increased by 11 pcm. Results of the measurement are summarized in Table II.

Table II: Excess reactivity of the core 133 with neutron source at different locations, $T_W = T_F = 22{,}5°C$

Source location	Safety rod location	ρ [pcm]
E-12	out	266
E-12	302	6
out	302	50
E-2	302	6
F-7	302	17

2.6 Thermal power calibration

The purpose of this measurement was to calibrate thermal power of the reactor for flux measurements in the next step. The flux measurement was performed at 1 - 2 kW so the calibration need not be very accurate. Water temperature was taken from the tank water temperature channel. It was measured for $\approx$ 2 h, increase of $\approx$ 2°C was observed, the temperature curve was linear. Thermal power of the reactor at which calibration was performed, was 28 kW. Linear channel signal was calibrated to 1.1 μA/kW. Accuracy of the measurement is estimated to be $\approx \pm$ 10 %.

2.7 Flux distribution measurements, core no. 133 A

The purpose of this measurement was experimental verification of flux and power peaking factors which were calculated for pulse analysis. Radial and axial flux distributions were measured using copper wires, gold and indium foils. Cadmium ratio was measured in some points as well. Copper was used for relative flux distribution measurements, while gold and indium (with or without Cd cover) were used for absolute thermal and epithermal flux determination. From the aspect of this report only relative power distributions are important. Copper samples fixed to aluminium probes were inserted into the holes in the upper plate which were provided for flux measurements. The locations of the holes allow measuring of two diametral distributions: first array of holes crosses transient and safety rod (array A), second array is 60° rotated with respect to the first one and does not cross control rod position (array B). Both arrays were used (see Fig. 1). Flux was measured approximately at the half-height of the active part of the fuel (8 cm long wires). At 8 locations Cu wire covered almost the entire height of the fuel elements to measure also the axial distribution (50 cm long wires). Irradiation was performed at 1 kW (array A) and at 2 kW (array B). Irradiation time was 1000 s in both cases. Excess reactivity was compensated by regulating and compensating rods. Each wire was cut in 2 cm long samples which were measured using Ge-Li spectrometer. Relative axial flux distributions averaged over all full length samples is presented in Fig. 2. Relative radial flux distribution over the core midplane is presented in Fig. 3.

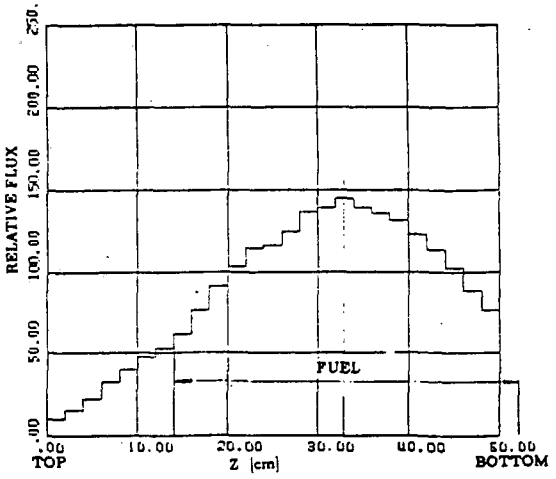

Fig. 2: Average axial relative flux distributions, core 133A, $\approx$ 1 kW

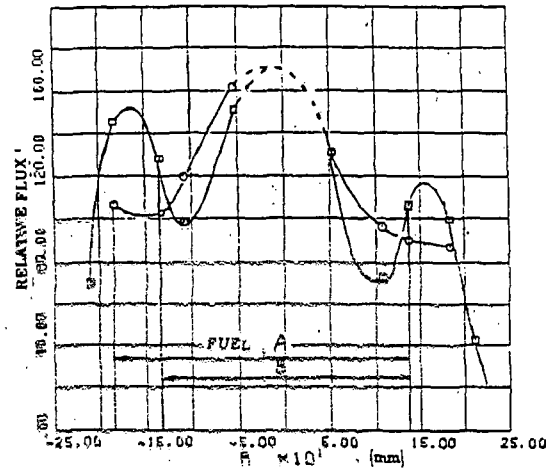

Fig. 3: Relative radial flux distribution, core 133A, ≈ 1 kW, circles array A, squares array B

The flux peaking factors calculated from distributions in Figs. 5 and 6 are presented in Table III. together with our predicted power peaking factors /1/.

Table III. Comparison of meaured flux peaking factors (core no. 133A, ≈1 kW) to power peaking factors from SAR

	meas. flux peaking fact.	calculated power peaking factor
radial	1.45 (in A ring)	1.39 (in B ring)
axial	1.31	1.25

The agreement between predicted and measured data is within error interval of the measurement (statistical error < 5%) and calculation (± 10 %). However, comparing the results the following effects must be taken into account:

- our previous experience shows that the flux distributions measured with copper as activation detector are superposition of thermal (80 %) and epithermal (20%) flux distributions due to relatively significant absorbtion cross-section of copper in the resonance region. Fast and epithermal flux radial distributions are more "peaked" than thermal. For this reason measured flux peaking factors are higher than power peaking factors which are proportional to thermal flux (fast fission in U-235 is negligible);
- flux is measured in water at locations between fuel elements. It is only roughly proportional to the flux in the fuel elements which is, however, proportional to the power distribution. Thermal flux at measuring locations depends on the size of the water gaps between fuel elements. Particularly large difference is between water gaps (cooling channels) near A and all others. During this experiment flux was not measured at the positions between rings A and B (mainly due to technical problems since the measuring holes in the grid plate between A and B are much smaller than the others and special probes had to be provided). The flux value at the centre of the core from which the peaking factor is calculated was not measured but only extrapolated from other measured points. Later measurements of the fuel element reactivity worth and flux distributions indicate that measured flux in ring A presented in Fig. 3 is overestimated and that actual power of the element at the centre is lower.

2.8 Increasing of excess reactivity

The purpose of this step was to increase excess reactivity of the core by adding fuel elements in E-ring. First, all elements in E-ring were reshuffled to the locations near control and regulating rods and then 5 new elements were added to form approximately symmetrical loading pattern (A, B, C, D all positions filled, E: 3, 2, 1, 24, 23, 22, 10, 11, 12, 13, 14, 15). Such configuration (core no. 134) was selected also to fill empty positions in triangular cutouts to provide stability of the fuel elements for power operation and pulsing. Excess reactivity $\rho = 2.7$ \$ was measured using safety rod calibration curve.

2.9 Control rod worth measurement

Control rod worths were measured again because the core configuration no. 134 was significantly different from the previous one (no. 133) for which the rod worths had been measured before. Both rod insertion and rod-swap method were used for all rods. Due to excess reactivity limitation, only 3 \$ worth of each rod was measured by swapping, while the rest had to be measured by insertion method. Results are presented in Table IV.

Table IV: Worth of control rods in core 134 measured by rod insertion and rod swap method, compared to core 133

	rod worth [pcm]	
Core 133	rod insertion	rod swap
R	1928	-
C	1539	-
S	5449	-
T	1918	-
Core 134		
R	3227	2551
C	2290	2429
S	3591	3430
T	2476	2262

Regulating rod was measured by swapping compensating rod and vice versa. Transient rod was measured by swapping safety rod and vice versa.

The same conclusions can be made as in the first rod worth measurement, particularly for the rod insertion measurement. Rod swap results seem more consistent, at least R and C rod worths are almost equal. However, the rod worths in this case significantly depend on the choice of the rod used for compensation. This is evident if we compare excess reactivity values measured by different rods (Table V).

Table V: Core 134 excess reactivity estimated from control rod critical positions and corresponding calibration curves of the regulating (R), compensating (C), safety (S) and transient (T) control rods

	Excess reactivity Average [pcm]		Deviation from average [%]			
			R	C	S	T
Rod Swap	(RCST)	2022	+ 6	+ 4	- 3	- 7
Rod Insertion	(CST)	1935	+ 29	0	- 7	+ 4

The statistical error in the control rod worth measurement by the rod swap method is small (< 5%) but the physical interpretation of the measurement is difficult because during the measurement of a particular control rod worth the reference core configuration is changing, since for every move of the measured control rod, another control rod has to be repositioned to compensate the change in reactivity. This control rod interference effect is reflected in the different estimates of excess reactivity from the critical control rod positions presented in Table V. The effect is

well known for power reactors, but it is larger than expected for the small TRIGA core. Note the large discrepancy in the excess reactivity estimated from the calibration curve of the regulating rod which enters the core very close to the detector. It is caused by the flux redistribution effect which is not compensated for.

Note also that the differential control rod worth measured by the rod swap method is practically exact when the reactor is operated with a control rod configuration, similar to the one used in the rod swap measurement. However, for estimating the shut down margin it is not strictly correct.

2.10 Fuel element reactivity worth in different rings

The reactivity worth of fuel elements in different rings was measured in core 134. Fuel element reactivity worth was measured from the difference in the regulating rod critical position (rod swap curve) before and after the fuel element was withdrawn from the core. As all elements were fresh and presumably identical, the worths were measured by withdrawing different elements from selected locations in different rings. Only in case of A and B ring, the same element was used in both rings as initial results suggested differences between fuel elements. However, the exchange of the elements showed identical results at the same location proving that the design differences between the elements were negligible. Results are presented in Table VI.

Surprisingly, the fuel element reactivity worth in A ring is lower than in B and even C. This can not be explained by the error of the measurement ($\approx \pm .1$ \$) because the measurement was repeated several times and with different fuel elements. The only explanation is that the flux and its importance are lower at the centre than in the outer rings since the unit cell is smaller (contains less water). This is evident from the geometry of the core. The flux depression in A was confirmed also by flux measurements. The consequence of the flux depression is lower power in A ring and also smaller power peaking factor. A good indication for the flux distribution and for the peaking factor is the normalized fuel element reactivity worth distribution given in the second column of Table VI.

It may be concluded that power peaking occurs in the B ring. The value 1.40 and location of the peaking are in agreement with other measured and predicted power distributions. It is also important to note that reduced power in A compensates worse cooling of the central element, as can be seen from fuel temperature distribution measurements.

Table VI: Fuel element worth in different rings

Position	ρ [$]	ρ / average
A1	1.3	1.15
B2	1.5	
B3	1.6	1.40
B4	1.7	
B5	1.7	
C8	1.5	1.30
D11	1.05	
D13	1.05	.90
E14	.75	.65
average	1.15	

2.11 Thermal power calibration

Thermal power calibration of the core No.134 was performed. Water temperature was recorded on-line from 2 independent thermocuples, one at the top of the tank and one above the core. Periodically also water samples were measured as well. The purpose of the redundant measurements was to estimate the influence of temperature distribution on power calibration. However, all three independent measurements at different locations in the tank showed the same temperature increase and gave practically the same calibration results. Considering other inaccuracies (e.g. thermal capacity constant), the error of ± 10 % was estimated for thermal calibration method which is in use at our TRIGA reactor.

2.12 Void coefficient measurement

The purpose of this measurement was to show that the void coefficient was negative anywhere in the core. It was measured using Al probes which are normally used for flux measurements. $\Delta\rho$ was measured by reactivity computer. Values between - 400 pcm /(% void) near B ring and - 100 pcm/(% void) near E ring were measured.

2.13 Fuel temperature coefficient measurement

Fuel temperature coefficient α_f was measured by measuring fuel temperature increase after withdrawing regulating rod by ≈ 50 pcm (all other rods withdrawn

completely). Reactivity change was measured directly by reactivity computer and from the regulating rod position. Due to relatively small differences in rod position, a rather inaccurate rod position indication (± 1 or 2 steps) and an inappropriate regulating rod calibration curve (i.e., the calibration curve should correspond to all other rods withdrawn, but the only available was the rod-swap curve since the rod insertion curve is inaccurate for the regulating rod), the $\Delta\rho$ measurements from the rod position were not reliable. $\Delta\rho$ readings from reactivity meter exhibited significantly better accuracy, at least for small temperatures. Fuel temperature was measured in A and B ring. Like $\Delta\rho$, also ΔT readings became very inaccurate above ≈ 100°C, resulting in an error on α_f of up to ≈ 200%. Below 100°C the error is estimated to be ≈ ± 10%. The α_f, measured from $\Delta\rho$ and temperature in ring A or B (T_A or T_B) was transformed to the α_f of the reactor on average by transforming T_A or T_B into average fuel temperature $\overline{T}$ and using the formula:

$$\alpha_f\,(\overline{T}) = \gamma_z\,\beta_r\,\alpha_f\,(T_r), \qquad r = A, B$$

where

$$\gamma_r = \frac{T_r - T_o}{\overline{T} - T_o}, \qquad T_o = 22.5°C \tag{1}$$

γ_z is the ratio between the temperature at the axial location of the thermocouple and the axial average temperature, taking into account that the temperature is measured at the axial maximum and not at the average position. γ_z was estimated from the axial power distribution, $\gamma_z = 1.25$. β_r is a correction for the radial temperature distribution in the core. It was calculated from the measurements of fuel temperature in different rings in Fig. 6. T_A, T_B and $\overline{T}$ as functions of reactor power are presented in Fig. 4. $\alpha_f\,(T_A)$, $\alpha_f\,(T_B)$ and $\alpha_f\,(\overline{T})$ are presented in Fig.5. We see that at low temperature $\alpha_f\,(\overline{T})$ is ≈ -6 pcm/°C and grows to ≈ -10 pcm/°C at 100°C. Our calculations are in very good agreement at low temperature (-6 pcm/° at 20°C), but seem to be uderestimated at higher temperature (-7.5°C at 100°C). With respect to the pulse analysis this is conservative, i.e., smaller pulses may be expected at the same pulse reactivity.

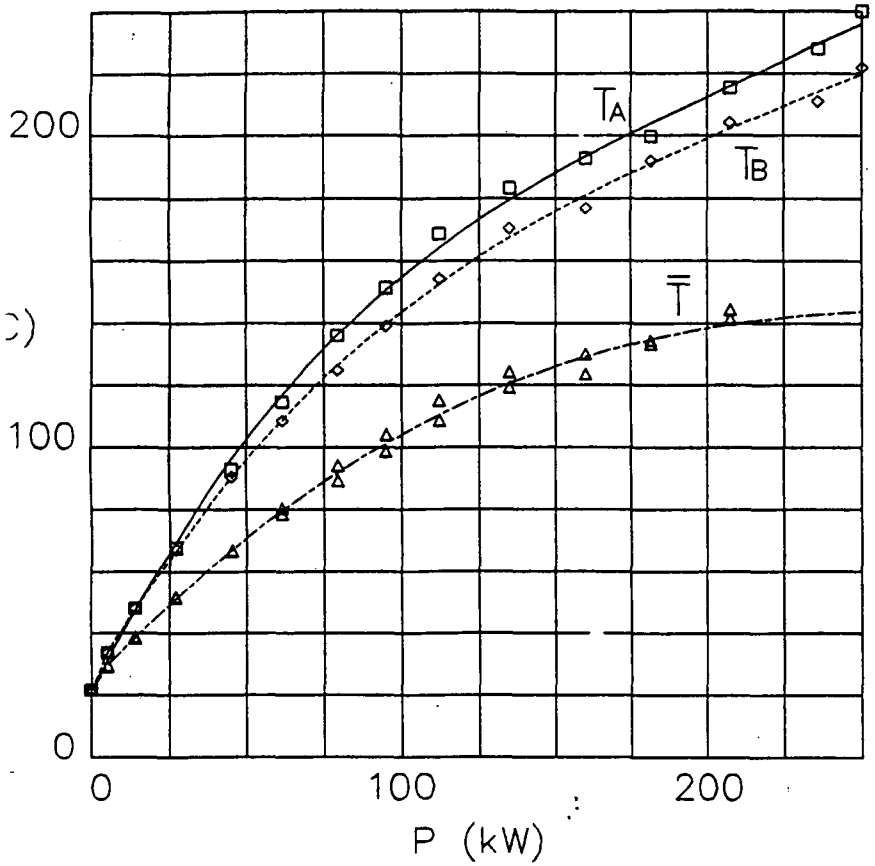

Fig. 4: Fuel temperature in rings A and B as a function of reactor power (T_A and T_B) and core average temperature ($\overline{T}$)

Power coefficient and power defect were measured as well. Relatively high power defect was measured (1.8 $ at 250 kW) due to relatively large specific power and consequently high fuel temperature, which both result from a smaller number of fuel elements in the core.

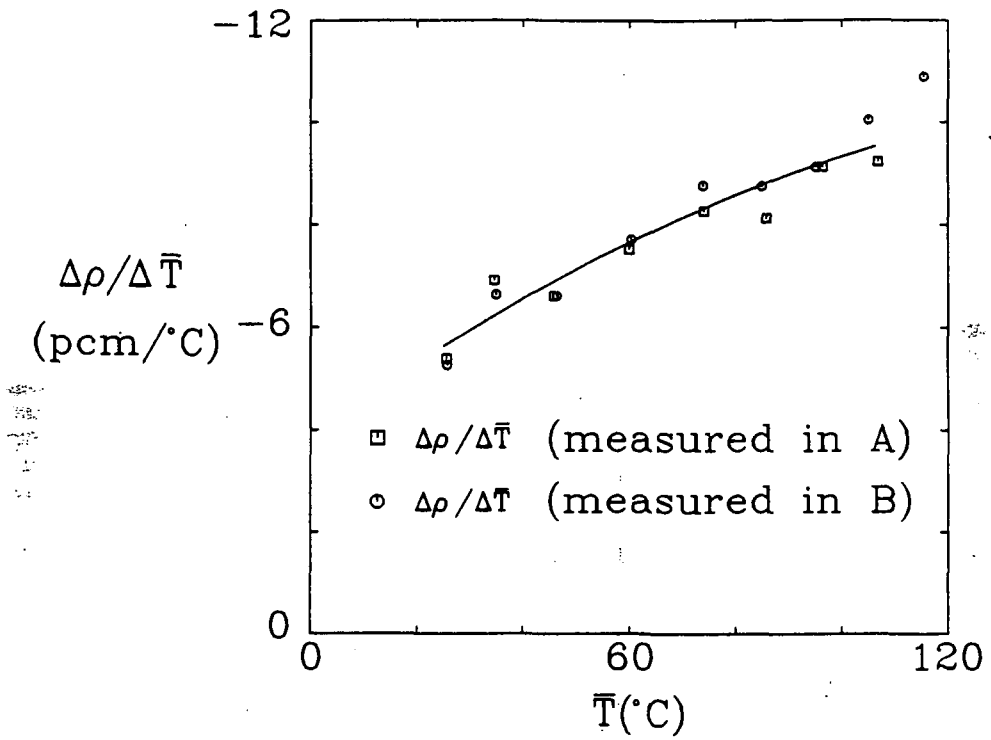

Fig.5: α_f ($\overline{T}$) dependence on average fuel temperature $\overline{T}$

2.14 Fuel temperature measurement in different rings

One of the instrumented fuel elements was reshuffled from its original location in B-5 to several different locations in different rings. Its temperature was measured at each location for 50% and 100% (250 kW) reactor power. Results are presented in Fig. 6.

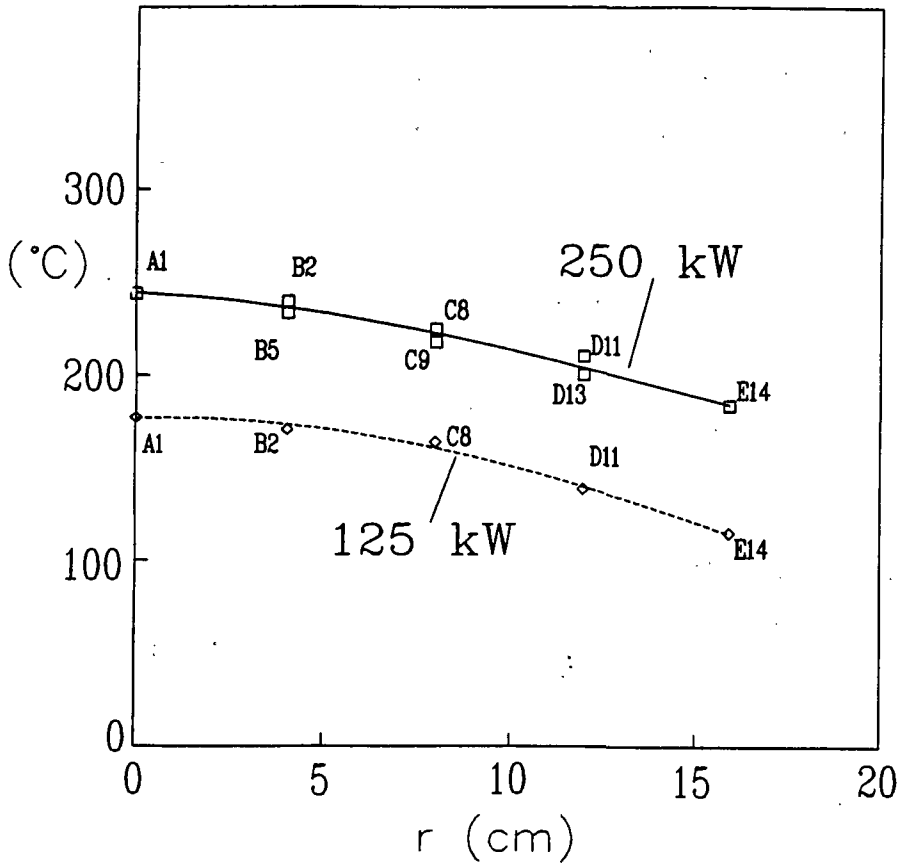

Fig. 6: Fuel temperature in different rings at 100% and 50% power

2.15 Flux distribution measurements

Flux distributions were measured for core 134. The same method was used as in previous steps (copper wire and gold foils). The novelty was measuring of the axial flux distribution in positions between A and B ring. Copper wire was fixed to special Al probes with ≈ 3 mm diameter. The purpose of this measurement was to check the flux depression at the centre which was indicated by fuel element worth and

temperature measurements. Results are presented in Fig. 7. Flux depression in the centre is clearly visible. Average fluxes in different rings are presented in Table VII. together with fuel element worths.

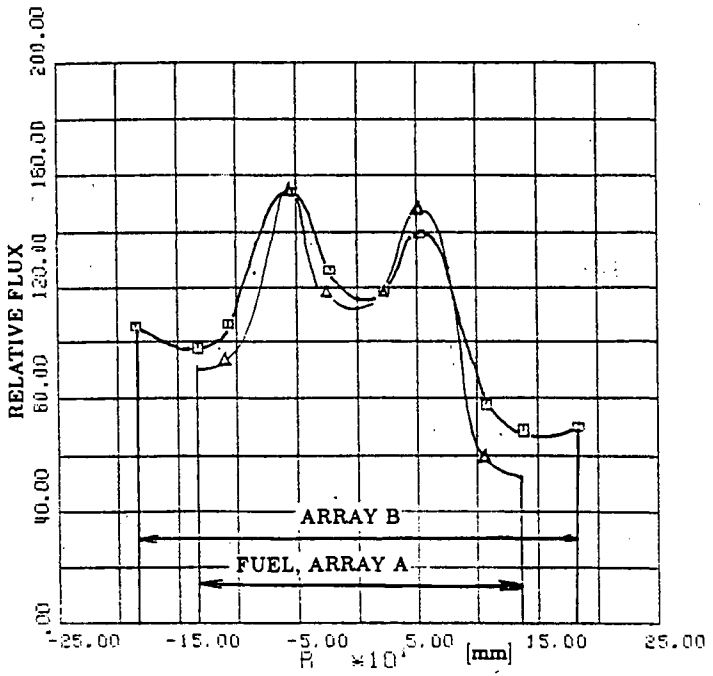

Fig. 7: Radial relative flux distribution, Core 134, ≈ 1 kW

Table VII: Ring averaged relative fluxes and relative fuel element reactivity worths, core 134

Ring	no. of elements	relative flux	relative worth
A	1	1.20	1.15
B	6	1.38	1.40
C	11	1.15	1.30
D	18 (-2 x .5 FF)	.83	.90
E	12	.94	.65

The agreement between two independent measurements confirms previous assumptions about radial power peaking factor. Power peaking occurs in B ring, the value is 1.40 ± .10. Relative power of the central fuel element is approximately the same as in C ring. However, it should be stressed again that flux is measured in water near fuel elements and that thermal flux in the fuel element is from 10 - 30% lower, depending on the size of the water gap. It is expected that the flux in the central element is less reduced with respect to water than for other elements, i.e., the depression in power distribution is not as strong as in the measured flux.

3 PULSE EXPERIMENTS

The pulses were performed from (slightly) subcritical reactor because the pulse rod worth was greater than the maximum allowable excess reactivity. Excess reactivity was measured at the beginning of the pulse experiments using transient rod for compensation. The rod insertion calibration curve was used for determining the transient rod worth and pulse reactivity. As it is pointed out in the previous text the rod insertion measurements correspond better to the transient rod worth for pulsing than rod swap method measurements. According to the rod insertion method, the core configuration during the measurement is constant so the effect of interference is less pronounced. Core configuration during the rod insertion measurements corresponds more closely to that during pulsing, especially for smaller pulses.

The total worth of the transient rod is 2476 pcm. Excess reactivity was measured to be 2146 pcm. The reactor was 330 pcm subcritical when the transient rod was completely inserted i.e., at the starting position for pulsing. The pulse reactivity ρ_i is calculated from the reactivity of the transient rod at specified position ρ_T reduced by 330 pcm.

Automatic logging of the nv channel signal on the process computer was provided using an ACD card with sampling time of approx. 10^{-5} s. Examples of the pulse power measurements are presented in Fig. 8. The maximal and integrated pulse power was read from the nv and nvt channel instruments directly. The pulse width was taken from the digitalized pulse signal. The results of the measurements are presented in Table VIII together with the calculated results which were obtained using the PULSTRI code for particular core configuration and pulse reactivity. Results are presented also in graphical from in Figs. 9-13.

Fig. 9 shows measured ($E_{t,D}$) and calculated ($E_{t,P}$) total energy in dependence of prompt reactivity ($\rho_i - \beta$). For small pulses ($\rho_i < 2$ \$), measured and calculated, results agree within ± 5 %. For $\rho_i > 2$ \$ the agreement is not so good but still within ± 20 %. The measurements show that the calculated total energy is overestimated. This is consistent with the results of α_f measurements. They show that the measured and calculated values of α_f agree well at low temperature, while at higher temperatures (> 150°C) measured α_f exceeds calculated results for approx. 20 % in absolute value (- 7.5 pm/°C calculated, -10 pcm/°C measured). However, the difference between predicted and measured E_t is small and conservative, i.e., the actual maximal temperatures are expected to be lower than those calculated.

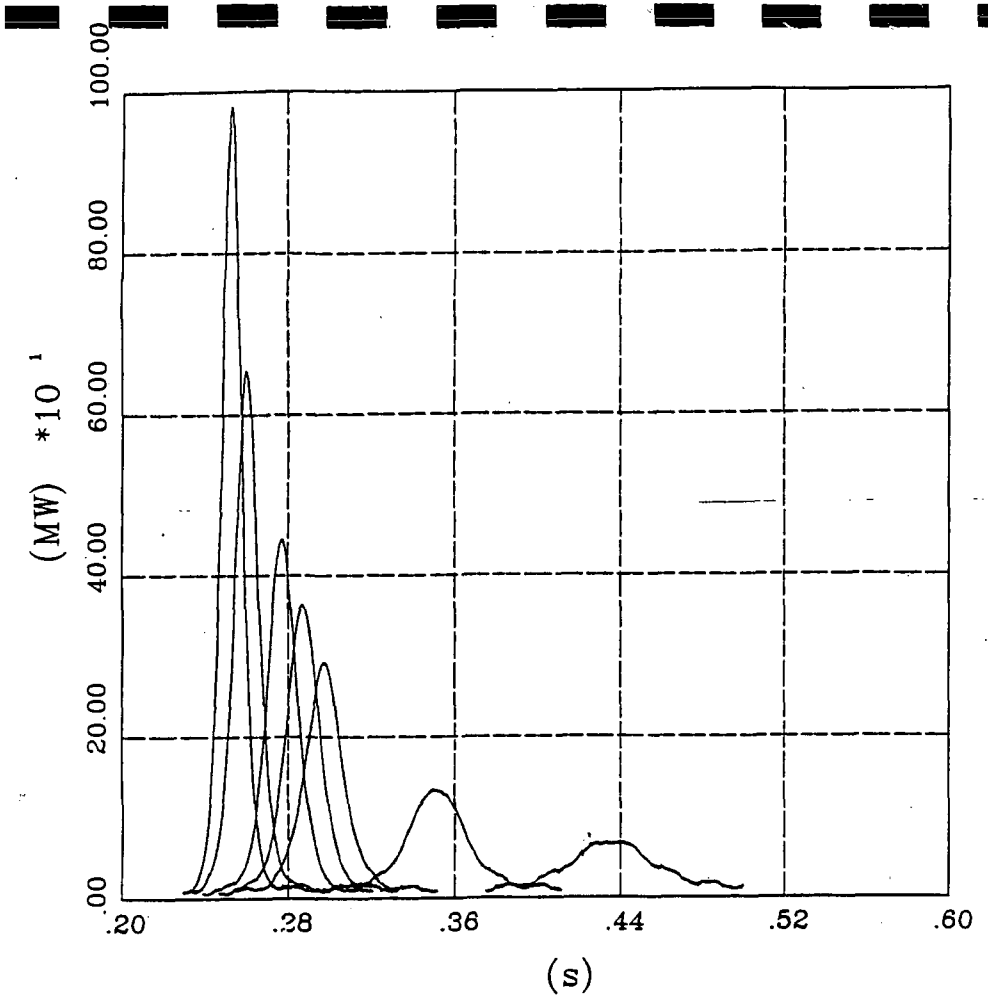

Fig. 8: Pulse power in dependence of time

Maximal measured fuel temperature as a function of prompt reactivity is presented in Fig. 10. It is compared to the calculated value, which was obtained by the PULSTRI code using the measured f_T value ($f_T = 1.9$) and the actual number of fuel elements (48). However it must be noted that the measured and the calculated temperatures can not be directly compared. The calculations imply that the power peaking occurs at the outer radius of the fuel rod while the measured temperature corresponds more to the fuel rod center line where the thermocouple sensors are located. For this reason the maximum of the measured temperature is also delayed in time, as can be seen from Fig. 11. The time delay is decreased with inserted reactivity (Fig. 12).

The maximal measured fuel temperature as a function of $(\rho_i - \beta)^2$ is presented in Fig. 13. The linearity of the curve is an indication that the ρ_i values are correct. If rod swap calibration curve is used instead of rod insertion for transient rod worth reading, the curve will not be linear and also the agreement with the PULSTRI calculations will be spoiled. The use of the rod insertion calibration curve for transient rod worths proves to be crucial for good quality of pulse parameter measurements.

Table VIII: Measured and calculated pulse parameters

Pulse No.	E_t [MWs] P	D	P_{max} [MW] P	D	Δ P [ms] C	P	T [°C] A,B	T [°C] D
003	4.6	5.1	80.9	60	49	51	251	204
004	9.1	9.1	314.6	270	20	25	298	241
005	6.3	6.8	152.6	120	32	37	264	230
006		5.1		60	50		240	204
007	11.1	11.0	467.3	440	16	21	312	268
008	13.2	12.0	661.0	645	13	17	348	292
009	15.3	13.7	880.7	870	11	15	277	313
010	16.0	13.9	974.2	970	11	15	388	324
011	10.1	9.8	386.7	350	18	22	304	258

E_t - total energy
P_{max} - maximal power
Δ P - pulse width
T - fuel temperature, measured in A, B and D ring
C - measured value (from the digitalized pulse record)
P - calculated with PULSTRI program
D - direct reading from NVT or NV channel instrument

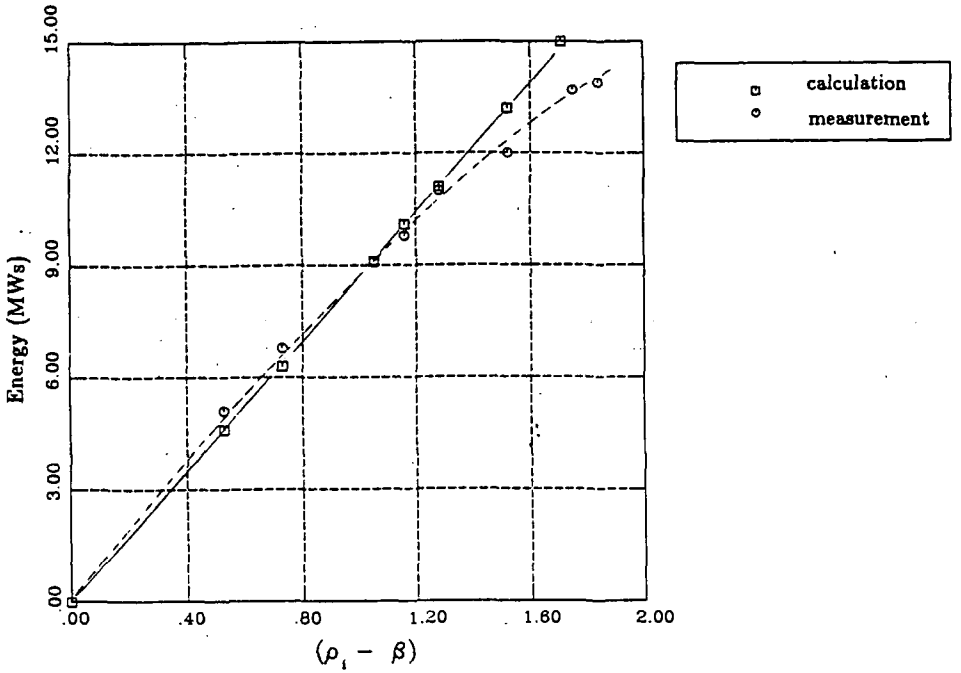

Fig. 9: Measured ($E_{t,D}$) and calculated ($E_{t,P}$) total energy in dependence of prompt reactivity (ρ_i - β)

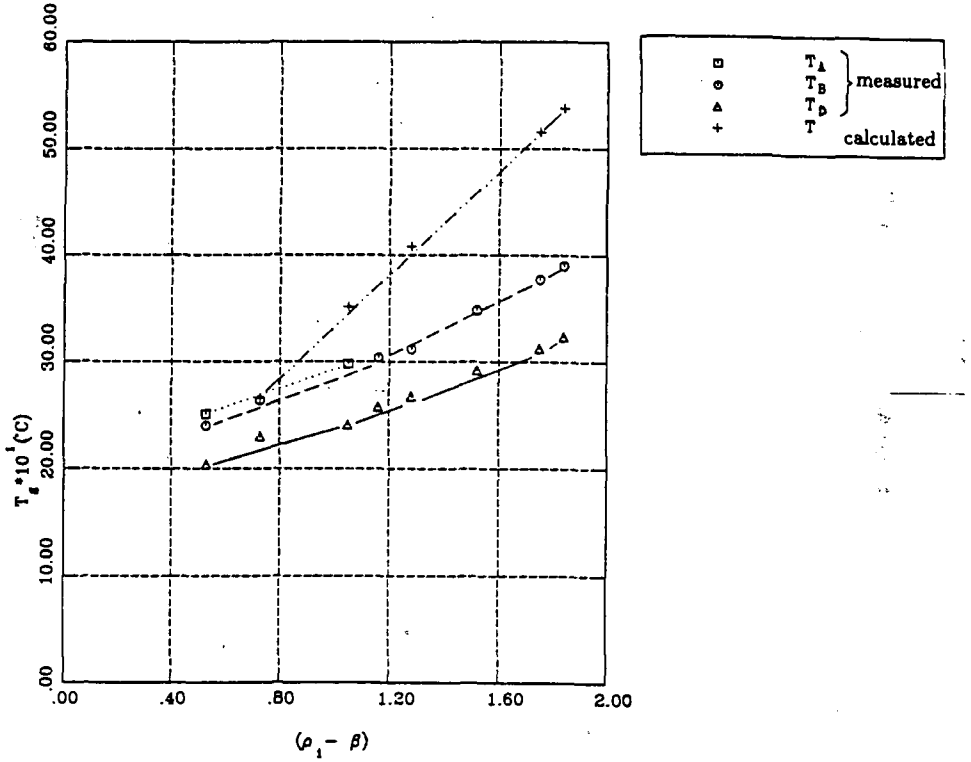

Fig. 10: Measured and calculated fuel temperature. Capital letters denote rings in which instrumented elements were located.

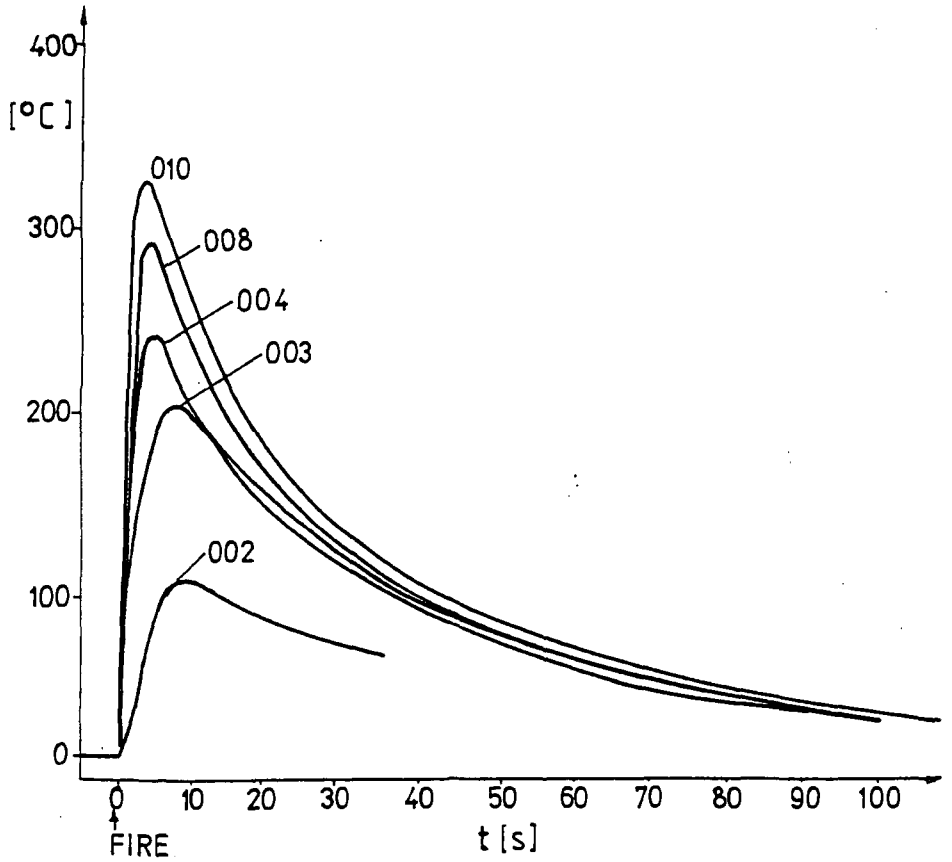

Fig. 11: Fuel temperature as a function of time after pulse (D ring).

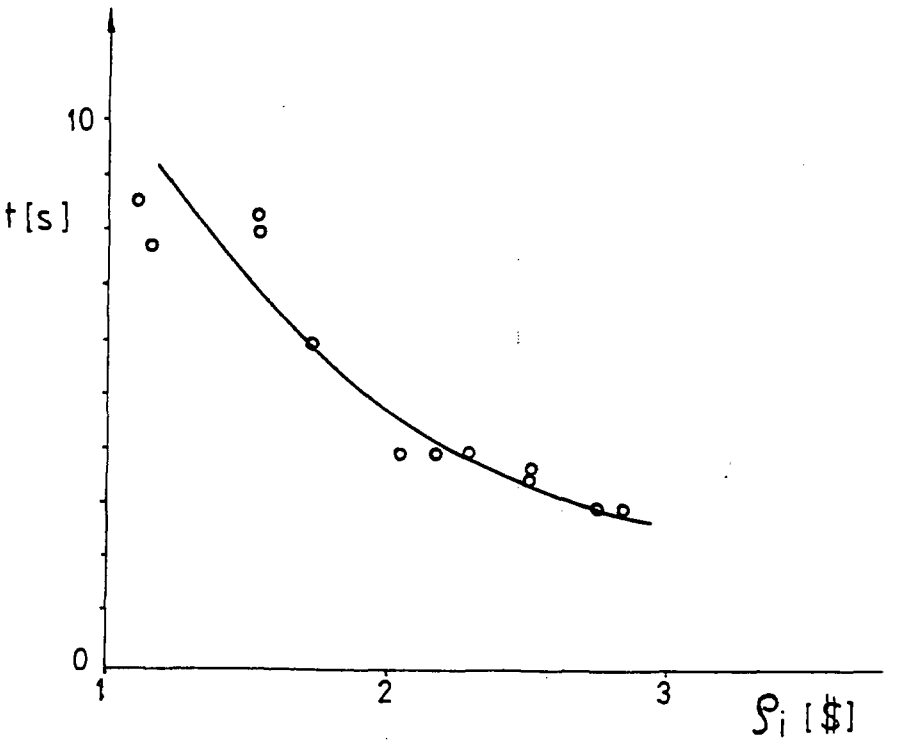

Fig. 12: Time delay of the measured temperature maximum in dependence of inserted reactivity.

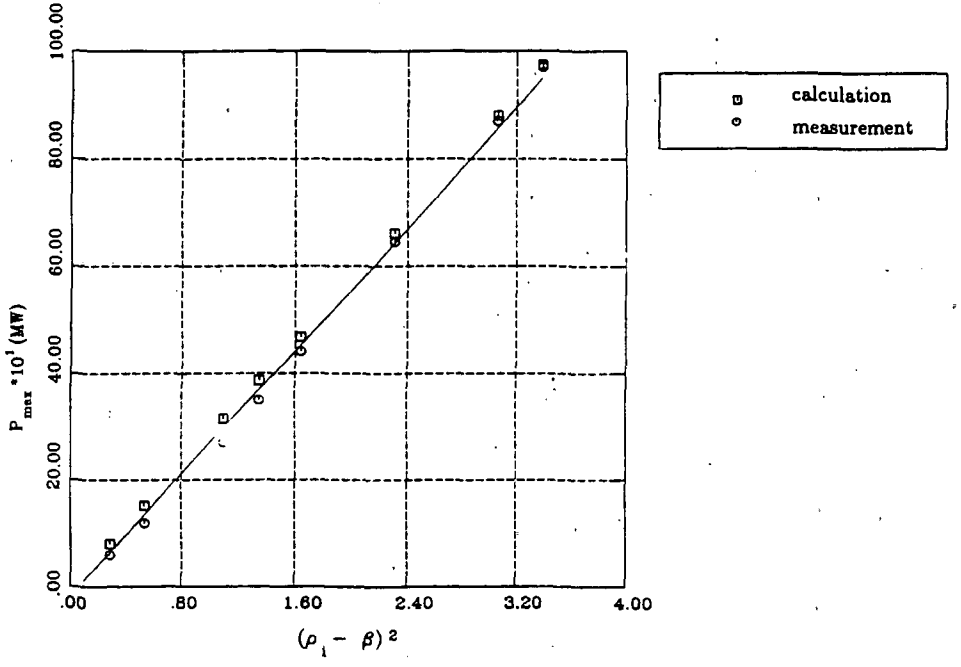

Fig. 13: Measured $P_{max,D}$ and calculated $P_{max,P}$ maximal pulse power as a function of $(\rho_i - \beta)^2$.

4 CONCLUSIONS

The main purpose of the reactor physics tests was to verify the predicted and calculated values for the most important reactor parameters which had been used in safety evaluation of pulse operation. It can be concluded, that the measured values well agree with the predicted:

parameter	predicted	measured
α_f, [pcm/°C], 20°C	- 6	- 6 ± .5
α_f, [pcm/°C], 100°C	- 7.5	- 10 ± 2
f_R	1.4	1.4 ± .1
f_Z	1.25	1.25 ± .1
pulse rod worth, [$]	> 3	3.2 ± .1
void coefficient	negative	negative

Comparison of measured results to the calculations show satisfactory agreement so as to qualify our computer codes and calculational procedures as analytical tools for evaluating the pulse experiments in future.

5 REFERENCES

/1/ Varnostno poročilo za reaktor TRIGA Mark II v Podgorici, Revizija 2, IJS-DP-5823, 29.maj 1991 (SAR, in Slovene)

/2/ A. Trkov, M. Ravnik, H. Böck, B. Glumac
Reactivity Measurements in Close-to-critical TRIGA Reactor Using a Digital Reactivity Meter, Kerntechnik, in press